WATER RESOURCES RESEARCH, VOL. 27, NO. 10, PAGES 2719–2733, OCTOBER 1991

Analytical Solutions for Solute Transport in Three-Dimensional Semi-infinite Porous Media

FEIKE J. LEIJ, TODD H. SKAGGS, AND MARTINUS TH. VAN GENUCHTEN

U.S. Salinity Laboratory, U.S. Department of Agriculture, Agricultural Research Service, Riverside, California

This paper presents several analytical solutions for three-dimensional solute transport in semi-infinite porous media with unidirectional flow using first-type (or concentration) and third-type (or flux) boundary conditions at the inlet location of the medium. The solutions may be used for predicting solute concentrations in homogeneous media, verification of more comprehensive numerical models, and laboratory or field determination of solute transport parameters. The transport equation incorporates terms accounting for advection, dispersion, zero-order production, and first-order decay. General solutions were derived for an arbitrary initial distribution and solute input with the help of Laplace, Fourier, and Hankel transforms. Specific solutions are presented for rectangular and circular solute inflow regions, as well as for solutes initially present in the form of parallelepipedal or cylindrical regions of the medium. The solutions were mathematically verified against simplified analytical solutions. Examples of concentration profiles are presented for several solute transport parameters using both first- and third-type boundary conditions. A mass balance constraint is defined based on a prescribed solute influx; the third-type condition is shown to conserve mass whereas the first-type condition was found to always overestimate resident solute concentrations in the medium.

INTRODUCTION

Concern about contamination of the subsurface environment has greatly stimulated research of solute transport phenomena in porous media. Subsurface transport is generally described with the advection-dispersion equation (ADE) which can be derived from mass balance principles. In the deterministic approach with constant transport parameters with respect to time and position the ADE is linear and explicit closed-form solutions can generally be derived. Many solutions for the ADE are now available for a large number of initial and boundary conditions for one-dimensional transport [e.g., *van Genuchten and Alves*, 1982] and a smaller number of conditions for two- and three-dimensional transport [*Cleary and Ungs*, 1978; *Carnahan and Remer*, 1984; *Javandel et al.*, 1984; *Wexler*, 1989]. Because of the large variability of flow and transport properties in the field, the often transient nature of the flow regime, and the nonideal nature of applicable initial and boundary conditions, the usefulness of analytical solutions is often limited and numerical methods may be needed. Still, analytical solutions remain useful for validating numerical results, for providing initial estimates of pollution scenarios, for sensitivity analyses to investigate the effect of various transport parameters, and for extrapolative purposes over large times or distances where the use of numerical models becomes impractical.

One common scenario for soil or groundwater contamination involves the migration of pollutants, via advection and dispersion, from a diffuse or bounded source at the soil surface, or from a buried source close to the soil surface, into the subsurface environment. To solve these cases analytically, we require the pore water velocity and the dispersion coefficients to be constant in time and space and assume the medium be semi-infinite in the direction of flow and infinite perpendicular to the flow direction.

This paper is not subject to U.S. copyright. Published in 1991 by the American Geophysical Union.

Paper number 91WR01912.

Compared to the large body of literature pertaining to analytical solutions for one-dimensional transport, relatively little attention has been paid to analytical solutions of the two- or three-dimensional ADE. Most studies involving multidimensional transport examine instantaneous solute injection into a semi-infinite or infinite medium [*Cleary*, 1973; *Kuo*, 1976; *Yeh and Tsai*, 1976; *Wilson and Miller*, 1978; *Prakash*, 1984]. Solutions of this type can be readily extended to continuous solute application over a finite time. Typically, the contaminant source (being a point, line, plane, or parallelepiped) is located at the origin of the coordinate system with flow parallel to the infinite horizontal coordinate (e.g., a river or aquifer). Solutions for heat flow problems can often be directly applied [e.g., *Moltyaner and Killey*, 1988] or readily adapted for such infinite systems. Several solutions have also been reported for cases where the solute is applied during a finite time at the flow inlet during a finite period of time [*Harleman and Rumer*, 1963; *Bruch and Street*, 1967; *Ogata*, 1969; *Shen*, 1976; *Sagar*, 1982; *Batu and van Genuchten*, 1990]. Most of these solutions assume a first- or concentration-type condition rather than a third- or flux-type condition which is more appropriate if volume-averaged concentrations are considered [*van Genuchten and Parker*, 1984; *Tang and Peaceman*, 1987; *Chen*, 1987]. A variety of mathematical techniques have been employed to derive these analytical solutions for multidimensional transport. Among them are Green's functions [*Yeh and Tsai*, 1976; *Lindstrom and Boersma*, 1989], separation of variables [*Bruch and Street*, 1967], Laplace transforms [*Chen*, 1987], and Fourier transforms [*Cleary*, 1973].

The main objective of this paper is to derive analytical solutions for the three-dimensional ADE during one-dimensional flow in a three-dimensional semi-infinite medium using a straightforward solution procedure. The transport equation consists of terms describing linear equilibrium adsorption, zero-order production and first-order decay. The ADE is solved subject to both first- and third-type inlet boundary conditions, and assuming arbitrary initial and inlet concentration distributions. Analytical solutions will be de-

TABLE 1. Notation for Laplace, Fourier, and Hankel Transforms

Operator	Variable Transformation
$\mathcal{L}_t[\ \ ] = \int_0^\infty \exp(-st)[\ \ ]\,dt$	$C(x, y, z, t) \rightarrow \bar{C}(x, y, z, s)$
$\mathcal{L}_x[\ \ ] = \int_0^\infty \exp(-px)[\ \ ]\,dx$	$\bar{C}(x, y, z, s) \rightarrow \bar{C}^x(p, y, z, s)$
$\mathcal{F}_{yz}[\ \ ] = \int_{-\infty}^\infty \int_{-\infty}^\infty \exp[i(\alpha y + \beta z)][\ \ ]\,dy\,dz$	$\bar{C}^x(p, y, z, s) \rightarrow \bar{C}^{xyz}(p, \alpha, \beta, s)$
$\mathcal{H}_0[\ \ ] = \int_0^\infty \sigma J_0(\sigma r)[\ \ ]\,dr$	$\bar{C}^x(p, r, s) \rightarrow \bar{C}^{xr}(p, \sigma, s)$

rived using several integral transforms to reduce the partial differential equation into simplified algebraic expressions. The approach is shown to be applicable to a broad class of transport problems. General solutions are derived for transport using Cartesian and cylindrical coordinate systems. The results are then used to obtain analytical solutions for five specific combinations of initial and boundary value concentration profiles.

Previous work has shown that analytical solutions for first- and third-type inlet conditions can be associated with flux- and volume-averaged concentrations, respectively [*van Genuchten and Parker*, 1984]. Hence we shall derive here solutions for both types of conditions, although concentrations in this study are always assumed to be volume-averaged unless stated otherwise. A secondary objective of this paper is to investigate mass balance errors resulting from the use of inappropriate boundary conditions. This secondary objective is an extension of the work by *Batu and van Genuchten* [1990] who showed that analytical solutions for a third-type condition preserves mass in case of volume-averaged concentrations. These authors did not provide expressions for mass balance errors when a first-type condition was invoked.

MATHEMATICAL APPROACH

Cartesian Coordinates

Transport of a solute, subject to linear retardation and zero- and first-order rate processes, in a homogeneous and isotropic medium during one-dimensional steady state flow with three-dimensional dispersion is given by [e.g., *Bear*, 1979]:

$$R\frac{\partial C}{\partial t} = D_x\frac{\partial^2 C}{\partial x^2} - v\frac{\partial C}{\partial x} + D_y\frac{\partial^2 C}{\partial y^2} + D_z\frac{\partial^2 C}{\partial z^2} - \mu C + \lambda \tag{1}$$

$$t > 0,\quad 0 < x < \infty,\quad -\infty < y < \infty,\quad -\infty < z < \infty$$

where R is the retardation factor; C is the resident solute concentration (ML^{-3}); t is time (T); x is the position (L) in the direction of flow; y and z are rectangular coordinates perpendicular to the flow direction (L); D_x, D_y, and D_z are dispersion coefficients (L^2T^{-1}) in the x, y, and z directions, respectively; v is the pore water velocity (LT^{-1}); μ is a general first-order rate coefficient for decay (T^{-1}); and λ is a general zero-order rate coefficient for production ($ML^{-3}T^{-1}$).

The initial and boundary conditions are

$$C(x, y, z, 0) = f(x, y, z) \tag{2}$$

$$\left(vC - \delta D_x\frac{\partial C}{\partial x}\right)\bigg|_{x=0^+} = vg(y, z, t)$$

$$\delta = 0 \quad \text{first type} \qquad \delta = 1 \quad \text{third type} \tag{3}$$

$$\frac{\partial C}{\partial x}(\infty, y, z, t) = 0 \tag{4}$$

$$\frac{\partial C}{\partial y}(x, \pm\infty, z, t) = 0 \tag{5}$$

$$\frac{\partial C}{\partial z}(x, y, \pm\infty, t) = 0 \tag{6}$$

where f and g are arbitrary concentration profiles that will be specified later to illustrate pertinent transport problems.

The solution of (1), subject to (2) through (6), was achieved using Laplace transforms with respect to x and t and a double Fourier transform with respect to y and z. This procedure combines the solution technique for the one-dimensional ADE employed by *Lindstrom and Boersma* [1971] and the use of multiple integral transforms for multidimensional transport problems [cf. *Leij and Dane*, 1990]. Table 1 lists the various integral transforms used for solving the above problem, as well as the Hankel transform, $\mathcal{H}_0$, which will be used later for cylindrical coordinate systems. Note that p and s in Table 1 are the Laplace variables for x and t, respectively, and that α and β are Fourier transform variables for y and z, respectively. Detailed discussions of these transforms are given by *Spiegel* [1965] and *Sneddon* [1972], among others.

Application of the Laplace operator with respect to t and use of initial condition (2), results in the following transformation of (1):

$$R(s\bar{C} - f) = D_x\frac{\partial^2 \bar{C}}{\partial x^2} - v\frac{\partial \bar{C}}{\partial x} + D_y\frac{\partial^2 \bar{C}}{\partial y^2} + D_z\frac{\partial^2 \bar{C}}{\partial z^2} - \mu\bar{C} + \frac{\lambda}{s} \tag{7}$$

For brevity, the transforms of the accompanying boundary conditions are not given. The Laplace transform of (7) with respect to x, using condition (3), yields

$$R(s\bar{C}^x - f^x) = D_x\left\{p^2\bar{C}^x - (1-\delta)\left[p\bar{g} + \frac{\partial\bar{C}}{\partial x}(0, y, z, s)\right] - \delta p\bar{C}(0, y, z, s)\right\} + \nu[\bar{g} - p\bar{C}^x] + D_y\frac{\partial^2\bar{C}^x}{\partial y^2} + D_z\frac{\partial^2\bar{C}^x}{\partial z^2} - \mu\bar{C}^x + \frac{\lambda}{ps} \quad (8)$$

We proceed by applying the double Fourier transform. Assuming that $\bar{C}^x$ and its first derivative with respect to y and z vanish if $y \to \pm\infty$ or $z \to \pm\infty$, the Fourier transform of (8) is given by

$$R(s\bar{C}^{xyz} - f^{xyz}) = D_x\left\{p^2\bar{C}^{xyz} - (1-\delta)\cdot\left[p\bar{g}^{yz} + \frac{d\bar{C}^{yz}}{dx}(0, \alpha, \beta, s)\right] - \delta p\bar{C}^{yz}(0, \alpha, \beta, s)\right\} + \nu[\bar{g}^{yz} - p\bar{C}^{xyz}] - (\alpha^2 D_y + \beta^2 D_z)\bar{C}^{xyz} - \mu\bar{C}^{xyz} + \frac{\lambda^{yz}}{ps} \quad (9)$$

The following explicit expression for $\bar{C}^{xyz}$ can be readily derived [e.g., *Lindstrom and Boersma*, 1971]:

$$\bar{C}^{xyz}(p, \alpha, \beta, s) = \frac{1}{(p+A)^2 - B^2}\left\{(1-\delta)\left[p\bar{g}^{yz} + \frac{d\bar{C}^{yz}}{dx}(0, \alpha, \beta, s)\right] + \delta p\bar{C}^{yz}(0, \alpha, \beta, s) - \frac{1}{D_x}\left[\nu\bar{g}^{yz} + Rf^{xyz} + \frac{\lambda^{yz}}{ps}\right]\right\} \quad (10)$$

where

$$A = -\nu/(2D_x) \quad (11a)$$

$$B = [A^2 + (\alpha^2 D_y + \beta^2 D_z + Rs + \mu)/D_x]^{1/2} \quad (11b)$$

The transformed concentration is obtained directly from an algebraic equation (equation (10)) rather than a differential equation.

The concentration in the regular space-time domain is derived via subsequent inversions of the Laplace and Fourier domain solutions. First, we invert with respect to p by applying the operator $\mathcal{L}_x^{-1}$. Using the shifting property, the convolution theorem, and a table of Laplace transforms [*Spiegel*, 1965], we obtain

$$\bar{C}^{yz}(x, \alpha, \beta, s) = \frac{1}{B}[(1-\delta)\bar{g}^{yz} + \delta\bar{C}^{yz}(0, \alpha, \beta, s)] \cdot \exp(-Ax)[B\cosh(Bx) - A\sinh(Bx)] + \frac{1}{B}\left((1-\delta)\frac{d\bar{C}^{yz}}{dx}(0, \alpha, \beta, s) - \frac{\nu\bar{g}^{yz}}{D_x}\right) \cdot \exp(-Ax)\sinh(Bx) - \frac{R}{BD_x}\int_0^x\left[f^{yz}(\xi, \alpha, \beta) + \frac{\lambda^{yz}}{Rs}\right]\exp[-A(x-\xi)]\sinh[B(x-\xi)]\,d\xi \quad (12)$$

Next (4) is invoked to evaluate $\bar{C}^{yz}(0, \alpha, \beta, s)$ and $d\bar{C}^{yz}/dx(0, \alpha, \beta, s)$ as outlined in the appendix. The resulting expressions are substituted in (12), which in turn can be rewritten as

$$\bar{C}^{yz}(x, \alpha, \beta, s) = \frac{\exp[-x(A-B)]}{2BD_x}\int_x^\infty \vartheta\exp[\xi(A-B)]\,d\xi + \exp[-x(A+B)]\left\{\bar{g}^{yz}\left((1-\delta) + \frac{\delta\nu}{B-A}\right) + \frac{1}{2BD_x}\left[\int_0^x \vartheta\exp[\xi(A+B)]\,d\xi + \left(\delta\frac{B+A}{B-A} - (1-\delta)\right)\int_0^\infty \vartheta\exp[\xi(A-B)]\,d\xi\right]\right\} \quad (13)$$

where

$$\vartheta = Rf^{yz}(\xi, \alpha, \beta) + \frac{\lambda^{yz}}{s} \quad (14)$$

This solution is inverted to the real time domain by employing the operator $\mathcal{L}_t^{-1}$. Using the table of Laplace transforms by *van Genuchten and Alves* [1982] and evaluating A and B leads to

$$C^{yz}(x, \alpha, \beta, t) = \int_0^t g^{yz}(t-\tau, \alpha, \beta)\left\{(1-\delta)\frac{x}{\tau}\Psi_1(\tau) + \delta\frac{\nu}{R}\left[2\Psi_1(\tau) - \Psi_2(\tau)\,\mathrm{erfc}\left(\frac{Rx+\nu\tau}{(4RD_x\tau)^{1/2}}\right)\right]\right\}d\tau + \int_0^\infty\left\{f^{yz}(\xi, \alpha, \beta)[(1-\delta)\Psi_3(t)\Psi_1(t) + 2\delta\Psi_4(t)\Psi_1(t)] + \int_0^t\frac{\lambda^{yz}}{R}[(1-\delta)\Psi_3(\tau)\Psi_1(\tau) + 2\delta\Psi_4(\tau)\Psi_1(\tau)]\,d\tau\right\}d\xi - \delta\int_0^\infty\left\{f^{xy}\Psi_2(t)\,\mathrm{erfc}\left[\frac{R(x+\xi)+\nu t}{(4RD_x t)^{1/2}}\right] + \int_0^t\frac{\lambda^{yz}}{R}\Psi_2(\tau)\,\mathrm{erfc}\left[\frac{R(x+\xi)+\nu\tau}{(4RD_x\tau)^{1/2}}\right]d\tau\right\}d\xi \quad (15)$$

where

$$\Psi_1(\tau) = \left(\frac{R}{4\pi D_x\tau}\right)^{1/2} \exp\left(-\frac{Rx^2 - 2\nu x\tau}{4D_x\tau} - \gamma\tau\right) \quad (16a)$$

$$\Psi_2(\tau) = \frac{\nu}{2D_x} \exp\left(-\frac{\nu^2\tau + 4R\nu x}{4RD_x} - \gamma\tau\right) \quad (16b)$$

$$\Psi_3(\tau) = \exp\left(-\frac{R\xi^2 + 2\nu\xi\tau}{4D_x\tau}\right) \sinh\left(\frac{Rx\xi}{2D_x\tau}\right) \quad (16c)$$

$$\Psi_4(\tau) = \exp\left(-\frac{R\xi^2 + 2\nu\xi\tau}{4D_x\tau}\right) \cosh\left(\frac{Rx\xi}{2D_x\tau}\right) \quad (16d)$$

$$\gamma = [\nu^2 + 4D_x(\alpha^2 D_y + \beta^2 D_z + \mu)]/(4RD_x) \quad (17)$$

Finally, the inverse Fourier operator is applied. We will use the convolution theorem for the Fourier transform:

$$\mathcal{F}_{yz}^{-1}[g^{yz}(t-\tau, \alpha, \beta) \exp(-\gamma\tau)] = \exp\left(-\frac{\nu^2\tau}{4D_x} - \frac{\mu\tau}{R}\right) \cdot \frac{1}{2\pi}\int_{-\infty}^{\infty}\int_{-\infty}^{\infty} \frac{g(t-\tau, y-\nu, z-\eta)}{(4D_yD_z\tau^2)^{1/2}} \cdot \exp\left(-\frac{\nu^2}{4D_y\tau} - \frac{\eta^2}{4D_z\tau}\right) d\nu\, d\eta \quad (18)$$

where ν and η are dummy variables. Application of (18) leads to the following general solution:

$$C(x, y, z, t) = \int_0^t \int_{-\infty}^{\infty}\int_{-\infty}^{\infty} g(t-\tau, y-\nu, z-\eta)\Phi_1(\tau) \cdot \left\{\left(\frac{R}{\pi D_x\tau}\right)^{1/2} \exp\left(-\frac{(Rx-\nu\tau)^2}{4RD_x\tau}\right)\left[(1-\delta)\frac{x}{2\tau} + \delta\frac{\nu}{R}\right] - \delta\frac{\nu^2}{2RD_x}\exp\left(\frac{\nu x}{D_x}\right)\operatorname{erfc}\left[\frac{Rx+\nu\tau}{(4RD_x\tau)^{1/2}}\right]\right\} d\eta\, d\nu\, d\tau$$
$$+ \int_0^{\infty}\int_{-\infty}^{\infty}\int_{-\infty}^{\infty}\left\{\Phi_1(t) f(\xi, y-\nu, z-\eta) \cdot \left[\Phi_2(t)\left((1-\delta)\sinh\left(\frac{Rx\xi}{2D_xt}\right) + \delta\cosh\left(\frac{Rx\xi}{2D_xt}\right)\right) - \delta\frac{\nu}{2D_x}\exp\left(\frac{\nu x}{D_x}\right)\operatorname{erfc}\left(\frac{R(x+\xi)+\nu t}{(4RD_xt)^{1/2}}\right)\right]\right.$$
$$\left. + \int_0^t \frac{\lambda(y-\nu, z-\eta)}{R}\Phi_1(\tau)\left[\Phi_2(\tau)\left((1-\delta) \cdot \sinh\left(\frac{Rx\xi}{2D_x\tau}\right) + \delta\cosh\left(\frac{Rx\xi}{2D_x\tau}\right)\right) - \delta\frac{\nu}{2D_x}\exp\left(\frac{\nu x}{D_x}\right) \cdot \operatorname{erfc}\left(\frac{R(x+\xi)+\nu\tau}{(4RD_x\tau)^{1/2}}\right)\right] d\tau\right\} d\eta\, d\nu\, d\xi \quad (19)$$

where

$$\Phi_1(\tau) = \frac{R}{4\pi\tau(D_yD_z)^{1/2}} \exp\left(-\frac{\mu\tau}{R} - \frac{R\nu^2}{4D_y\tau} - \frac{R\eta^2}{4D_z\tau}\right) \quad (20a)$$

$$\Phi_2(\tau) = \left(\frac{R}{\pi D_x\tau}\right)^{1/2} \exp\left(-\frac{(Rx-\nu\tau)^2}{4RD_x\tau} - \frac{R\xi^2 + 2\nu\xi\tau}{4D_x\tau}\right) \quad (20b)$$

and where erfc denotes the complementary error function.

Cylindrical Coordinates

If the solute is applied from a circular source or if the solute is initially present in a cylindrical part of the medium, it is convenient to rewrite (1) in cylindrical coordinates:

$$R\frac{\partial C}{\partial t} = D_x\frac{\partial^2 C}{\partial x^2} - \nu\frac{\partial C}{\partial x} + \frac{D_r}{r}\frac{\partial}{\partial r}\left[r\frac{\partial C}{\partial r}\right] - \mu C + \lambda$$
$$t > 0,\ 0 < x < \infty,\ 0 < r < \infty \quad (21)$$

where x remains the direction of flow, and r is the cylindrical coordinate perpendicular to the flow direction. The transformation from (1) to (21) makes the assumption that transverse dispersion in any direction can be characterized by the same transverse dispersion coefficient, D_r. By contrast, (1) is more flexible by allowing different values for the transverse dispersion coefficients, D_y and D_z. The solution domain is now defined by ($x \geq 0$; $r \geq 0$). The initial boundary conditions are

$$C(x, r, 0) = f(x, r) \quad (22)$$

$$\left(\nu C - \delta D_x\frac{\partial C}{\partial x}\right)\bigg|_{x=0^+} = \nu g(r, t) \qquad \begin{matrix}\delta = 0 & \text{first type}\\ \delta = 1 & \text{third type}\end{matrix} \quad (23)$$

$$\frac{\partial C}{\partial x}(\infty, r, t) = 0 \quad (24)$$

$$\frac{\partial C}{\partial r}(x, \infty, t) = 0 \quad (25)$$

The solution procedure for this problem resembles the methodology for Cartesian coordinates. Again, the Laplace transforms with respect to x and t are used but instead of using a Fourier transform the zero-order Hankel transform with respect to r is applied. The latter transform is listed in Table 1, where $\mathbf{J}_0$ denotes the Bessel function of the first kind of order zero and σ is the transformation variable. Since the Hankel and Fourier transforms are quite similar, many of the results for Cartesian coordinates can be directly applied to the solution of the ADE for cylindrical coordinates. For our conditions, using the definition of the Hankel transform and integrating by parts, we have

$$\mathcal{H}_0\left[\frac{1}{r}\frac{d}{dr}\left(r\frac{d\bar{C}^x}{dr}\right)\right] = -\sigma^2\bar{C}^{xr} \quad (26)$$

Application of the two Laplace transforms and the Hankel transform leads to

$$\bar{C}^{xr}(p, \sigma, s) = \frac{1}{(p+A)^2 - E^2}\left[(1-\delta)\left(p\bar{g}^r + \frac{d\bar{C}^r}{dx}(0, \sigma, s)\right) + \delta p\bar{C}^r(0, \sigma, s) - \frac{1}{D_x}\left(\nu\bar{g}^r + Rf^{xr} + \frac{\lambda^r}{ps}\right)\right] \quad (27)$$

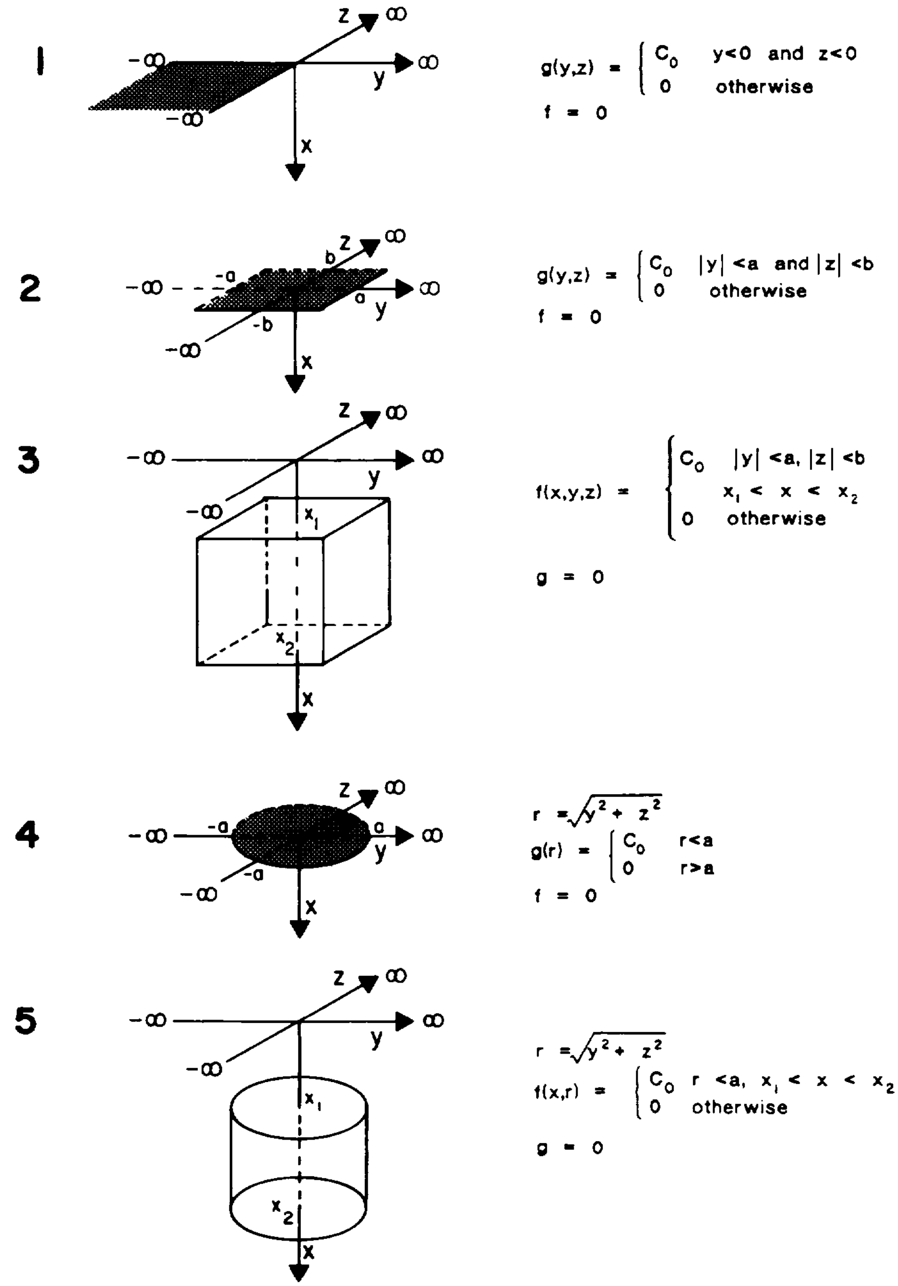

Fig. 1. Schematic of inlet and initial solute distributions for five selected cases: (1) diffuse source in quadrant of soil surface, (2) rectangular source at the soil surface, (3) parallelepipedal initial distribution, (4) circular source at the soil surface, (5) cylindrical initial distribution.

with

$$E = [A^2 + (\sigma^2 D_r + Rs + \mu)/D_x]^{1/2} \tag{28}$$

The Laplace inversions are similar to those for the Cartesian coordinates and results analogous to (13) and (15) were obtained. The Hankel inversion needs to be applied to all terms containing $g^r(t-\tau, \sigma)$, $f^r(\xi, \sigma)$, and λ^r. The inversion operator is formally written as

$$\mathcal{H}_0^{-1}[\ \ ] = \int_0^\infty [\ \ ]\sigma J_0(\sigma r)\, d\sigma \tag{29}$$

Consider the inversion of the $g^r(t-\tau, \sigma)$ term. Substitution of this term into (29) and evaluating the ensuing integral according to *Carslaw and Jaeger* [1959, p. 460], yields

$$\int_0^\infty g^r(t-\tau, \sigma) \exp\left(-\frac{\sigma^2 D_r \tau}{R}\right)\sigma J_0(\sigma r)\, d\sigma$$
$$= \int_0^\infty \frac{Rg(t-\tau, \rho)}{2D_r\tau} \exp\left(-\frac{R(r^2+\rho^2)}{4D_r\tau}\right) \mathrm{I}_0\left(\frac{Rr\rho}{2D_r\tau}\right)\rho\, d\rho \tag{30}$$

where I_0 denotes the modified or hyperbolic Bessel function of the first kind of order zero, and ρ is a dummy variable. Equation (30) can be directly applied to the inversion of the terms containing $f^r(\xi, \sigma)$ and λ^r. The general solution can now be written as

TABLE 2a. Analytical Solutions for Selected Transport Problems

Case	$C(x, y, z, t)$ or $C(x, r, t)$ First Type (F)	Third Type (T)
1	$\frac{C_0}{4}\int_0^t \frac{x}{\tau}\Lambda_1(\tau)\Gamma_1(\tau)\,d\tau + \frac{\lambda}{2R}\int_0^t \Lambda_2(\tau)\,d\tau$	$\frac{C_0}{4}\int_0^t \frac{\nu}{R}\Lambda_3(\tau)\Gamma_1(\tau)\,d\tau + \frac{\lambda}{2R}\int_0^t \Lambda_4(\tau)\,d\tau$
2	$\frac{C_0}{4}\int_0^t \frac{x}{\tau}\Lambda_1(\tau)\Gamma_2(\tau)\,d\tau + \frac{\lambda}{2R}\int_0^t \Lambda_2(\tau)\,d\tau$	$\frac{C_0}{4}\int_0^t \frac{\nu}{R}\Lambda_3(\tau)\Gamma_2(\tau)\,d\tau + \frac{\lambda}{2R}\int_0^t \Lambda_4(\tau)\,d\tau$
3	$\frac{C_0}{8}\Lambda_5(t)\Gamma_2(t) + \frac{\lambda}{2R}\int_0^t \Lambda_2(\tau)\,d\tau$	$\frac{C_0}{8}\Lambda_6(t)\Gamma_2(t) + \frac{\lambda}{2R}\int_0^t \Lambda_4(\tau)\,d\tau$
4	$2C_0\int_0^t\int_0^a \frac{x}{\tau}\Lambda_1(\tau)\Xi(\rho,\tau)\,d\rho\,d\tau + \frac{\lambda}{2R}\int_0^t\int_0^\infty \Lambda_2(\tau)\Xi(\rho,\tau)\,d\rho\,d\tau$	$2C_0\int_0^t\int_0^a \frac{\nu}{R}\Lambda_3(\tau)\Xi(\rho,\tau)\,d\rho\,d\tau + \frac{\lambda}{R}\int_0^t\int_0^\infty \Xi(\rho,\tau)\Lambda_4(\tau)\,d\rho\,d\tau$
5	$C_0\int_0^a \Lambda_5(t)\Xi(\rho,t)\,d\rho + \frac{\lambda}{2R}\int_0^t\int_0^\infty \Lambda_2(\tau)\Xi(\rho,\tau)\,d\rho\,d\tau$	$C_0\int_0^a \Lambda_6(t)\Xi(\rho,t)\,d\rho + \frac{\lambda}{2R}\int_0^t\int_0^\infty \Xi(\rho,\tau)\Lambda_4(\tau)\,d\rho\,d\tau$

See Table 2b for parameters.

$$C(x, r, t) = \int_0^t \int_0^\infty g(t-\tau, \rho)\Xi(\rho, \tau) \cdot \left\{ \left(\frac{R}{\pi D_x \tau}\right)^{1/2} \exp\left(-\frac{(Rx-\nu\tau)^2}{4RD_x\tau}\right)\left[(1-\delta)\frac{x}{\tau} + \delta\frac{2\nu}{R}\right] - \delta\frac{\nu^2}{RD_x}\exp\left(\frac{\nu x}{D_x}\right)\operatorname{erfc}\left[\frac{Rx+\nu\tau}{(4RD_x\tau)^{1/2}}\right]\right\} d\rho\, d\tau$$
$$+ \int_0^\infty \int_0^\infty \left\{ f(\xi, \rho)\Xi(\rho, t)\left[\Phi_2(t)\left((1-\delta)\sinh\left(\frac{Rx\xi}{2D_xt}\right) + 2\delta\cosh\left(\frac{Rx\xi}{2D_xt}\right)\right) - \delta\frac{\nu}{D_x}\exp\left(\frac{\nu x}{D_x}\right) \cdot \operatorname{erfc}\left(\frac{R(x+\xi)+\nu t}{(4RD_xt)^{1/2}}\right)\right] + \int_0^t \frac{\lambda}{R}\Xi(\rho, \tau)\left[\Phi_2(\tau)\left((1-\delta) \cdot \sinh\left(\frac{Rx\xi}{2D_x\tau}\right) + 2\delta\cosh\left(\frac{Rx\xi}{2D_x\tau}\right)\right) - \delta\frac{\nu}{D_x} \cdot \exp\left(\frac{\nu x}{D_x}\right)\operatorname{erfc}\left(\frac{R(x+\xi)+\nu\tau}{(4RD_x\tau)^{1/2}}\right)\right] d\tau \right\} d\rho\, d\xi \quad (31)$$

where

$$\Xi(\rho, \tau) = \frac{\rho R}{4D_r\tau}\exp\left(-\frac{\mu\tau}{R} - \frac{R(r^2+\rho^2)}{4D_r\tau}\right) I_0\left(\frac{Rr\rho}{2D_r\tau}\right) \quad (32)$$

Note that we chose λ to be independent of position.

APPLICATIONS

Some Common Transport Problems

The previous general solutions were used to derive specific analytical solutions for several simple transport problems. Figure 1 illustrates five cases, three of which involve a Cartesian coordinate system, and two a cylindrical system. For cases 1, 2, and 4 the solute is applied over different inlet areas to an initially solute free medium, while for cases 3 and 5 solute free water is applied to a soil where the solute is initially distributed uniformly in a bounded region of the soil (i.e., a paralellepiped or a cylinder). Analytical expressions for the solute concentrations are obtained by substituting the expressions for f and g, specified in Figure 1, into (19) and (31). The solutions for the five cases, using first- or third-type boundary conditions, are listed in Table 2.

A number of integrals that were encountered during the derivation of the specific solutions in Table 2 were evaluated using the following property of the Laplace transform

$$\mathscr{L}^{-1}\left[\frac{\bar{f}(s)}{s}\right] = \int_0^t F(\tau)\,d\tau \quad (33)$$

and the table of Laplace transforms in *van Genuchten and Alves* [1982]. Other useful integrals are given by *Abramowitz and Stegun* [1970] (i.e., 7.4.33 and 35), whereas the remainder were evaluated numerically using Gauss-Chebyshev quadrature [*Leij et al.*, 1991]. The modified Bessel function, I_0, was obtained according to *Press et al.* [1986]. The computer program 3DADE to evaluate the solutions in Table 2 is available upon request.

The five examples are merely illustrations of how analytical solutions can be derived from the general solutions. Other examples, for example, pulse-type changes in the influent concentration or two-dimensional transport, can be treated in a similar manner. Transport problems with more complicated initial (f) and boundary (g) concentration distributions can also be solved using the general analytical solutions; however, the need for additional numerical integration may make direct numerical solution of the transport problem more attractive.

Validation and Examples

In an effort to verify the derivation and numerical evaluation of the analytical solutions presented in Table 2 some simple cases were examined qualitatively. Note that any consistent set of units can be used for the parameter values and that, unless specified otherwise, $R = 1$ and $\mu = \lambda = 0$. Furthermore, for the (two-dimensional) illustrations we ar-

TABLE 2b. Expressions for Parameters in Analytical Solutions in Table 2a

Parameter	Expression
$\Gamma_1(\tau)$	$\operatorname{erfc}\left[\frac{y}{(4D_y\tau/R)^{1/2}}\right]\operatorname{erfc}\left[\frac{z}{(4D_z\tau/R)^{1/2}}\right]$
$\Gamma_2(\tau)$	$\left[\operatorname{erfc}\left(\frac{y-a}{(4D_y\tau/R)^{1/2}}\right)-\operatorname{erfc}\left(\frac{y+a}{(4D_y\tau/R)^{1/2}}\right)\right]\left[\operatorname{erfc}\left(\frac{z-b}{(4D_z\tau/R)^{1/2}}\right)-\operatorname{erfc}\left(\frac{z+b}{(4D_z\tau/R)^{1/2}}\right)\right]$
$\Xi(\rho,\tau)$	$\frac{\rho R}{4D_r\tau}\exp\left(-\frac{R(r^2+\rho^2)}{(4D_r\tau)}\right)\mathrm{I}_0\left(\frac{Rr\rho}{2D_r\tau}\right)$
$\Lambda_1(\tau)$	$\left(\frac{R}{4\pi D_x\tau}\right)^{1/2}\exp\left(-\frac{\mu\tau}{R}-\frac{(Rx-\nu\tau)^2}{4RD_x\tau}\right)$
$\Lambda_2(\tau)$	$\exp\left(-\frac{\mu\tau}{R}\right)\left[\operatorname{erfc}\left(\frac{\nu\tau-Rx}{(4RD_x\tau)^{1/2}}\right)-\exp\left(\frac{\nu x}{D_x}\right)\operatorname{erfc}\left(\frac{Rx+\nu\tau}{(4RD_x\tau)^{1/2}}\right)\right]$
$\Lambda_3(\tau)$	$\exp\left(-\frac{\mu\tau}{R}\right)\left[\left(\frac{R}{\pi D_x\tau}\right)^{1/2}\exp\left(-\frac{(Rx-\nu\tau)^2}{4RD_x\tau}\right)-\frac{\nu}{2D_x}\exp\left(\frac{\nu x}{D_x}\right)\operatorname{erfc}\left(\frac{Rx+\nu\tau}{(4RD_x\tau)^{1/2}}\right)\right]$
$\Lambda_4(\tau)$	$\exp\left(-\frac{\mu\tau}{R}\right)\left[\operatorname{erfc}\left(\frac{\nu\tau-Rx}{(4RD_x\tau)^{1/2}}\right)+\left(1+\frac{\nu}{D_x}(x+\nu\tau/R)\right)\exp\left(\frac{\nu x}{D_x}\right)\operatorname{erfc}\left(\frac{Rx+\nu\tau}{(4RD_x\tau)^{1/2}}\right)-\left(\frac{4\nu^2\tau}{\pi RD_x}\right)^{1/2}\exp\left(-\frac{(Rx-\nu\tau)^2}{4RD_x\tau}\right)\right]$
$\Lambda_5(t)$	$\exp\left(-\frac{\mu\tau}{R}\right)\left\{\operatorname{erfc}\left(\frac{R(x-x_2)-\nu t}{(4RD_xt)^{1/2}}\right)-\operatorname{erfc}\left(\frac{R(x-x_1)-\nu t}{(4RD_xt)^{1/2}}\right)+\exp\left(\frac{\nu x}{D_x}\right)\left[\operatorname{erfc}\left(\frac{R(x+x_2)+\nu t}{(4RD_xt)^{1/2}}\right)-\operatorname{erfc}\left(\frac{R(x+x_1)+\nu t}{(4RD_xt)^{1/2}}\right)\right]\right\}$
$\Lambda_6(\tau)$	$\exp\left(-\frac{\mu\tau}{R}\right)\left\{\exp\left(\frac{\nu x}{D_x}\right)\left[\left(1+\frac{\nu}{D_x}(x+x_1+\nu t/R)\right)\operatorname{erfc}\left(\frac{R(x+x_1)+\nu t}{(4RD_xt)^{1/2}}\right)-\left(1+\frac{\nu}{D_x}(x+x_2+\nu t/R)\right)\operatorname{erfc}\left(\frac{R(x+x_2)+\nu t}{(4RD_xt)^{1/2}}\right)\right]+\operatorname{erfc}\left(\frac{R(x-x_2)-\nu t}{(4RD_xt)^{1/2}}\right)-\operatorname{erfc}\left(\frac{R(x-x_1)-\nu t}{(4RD_xt)^{1/2}}\right)+\left(\frac{4\nu^2t}{\pi RD_x}\right)^{1/2}\exp\left(\frac{\nu x}{D_x}\right)\left[\exp\left(-\frac{[R(x+x_2)+\nu t]^2}{4RD_xt}\right)-\exp\left(-\frac{[R(x+x_1)+\nu t]^2}{4RD_xt}\right)\right]\right\}$

bitrarily used y for the transverse coordinate; identical results would have been obtained if z were used for this purpose.

First, the part of the solution that depends on x (i.e., the effect of longitudinal dispersion and advection) is investigated. This is done for a rectangular coordinate system where solute is applied over the entire soil surface (i.e., case 2 with a and $b \to \infty$), or where solute is incorporated in an infinite layer between x_1 and x_2 (i.e., case 3 with a and $b \to \infty$). The problem is in effect one-dimensional and analytical solutions are readily available. Indeed, the resulting expressions for case 2 (F2 and T2, where F denotes "first-type" and T "third-type" solution) are identical to solutions A1 and A2 by *van Genuchten and Alves* [1982] while the expressions for cases F3 and T3 correspond to solutions A5 and A6 by van Genuchten and Alves. Furthermore, we checked whether first- and third-type solutions obey the proper transformation in the concentration mode. As discussed by *van Genuchten and Parker* [1984] the use of a third-type condition for volume-averaged concentrations

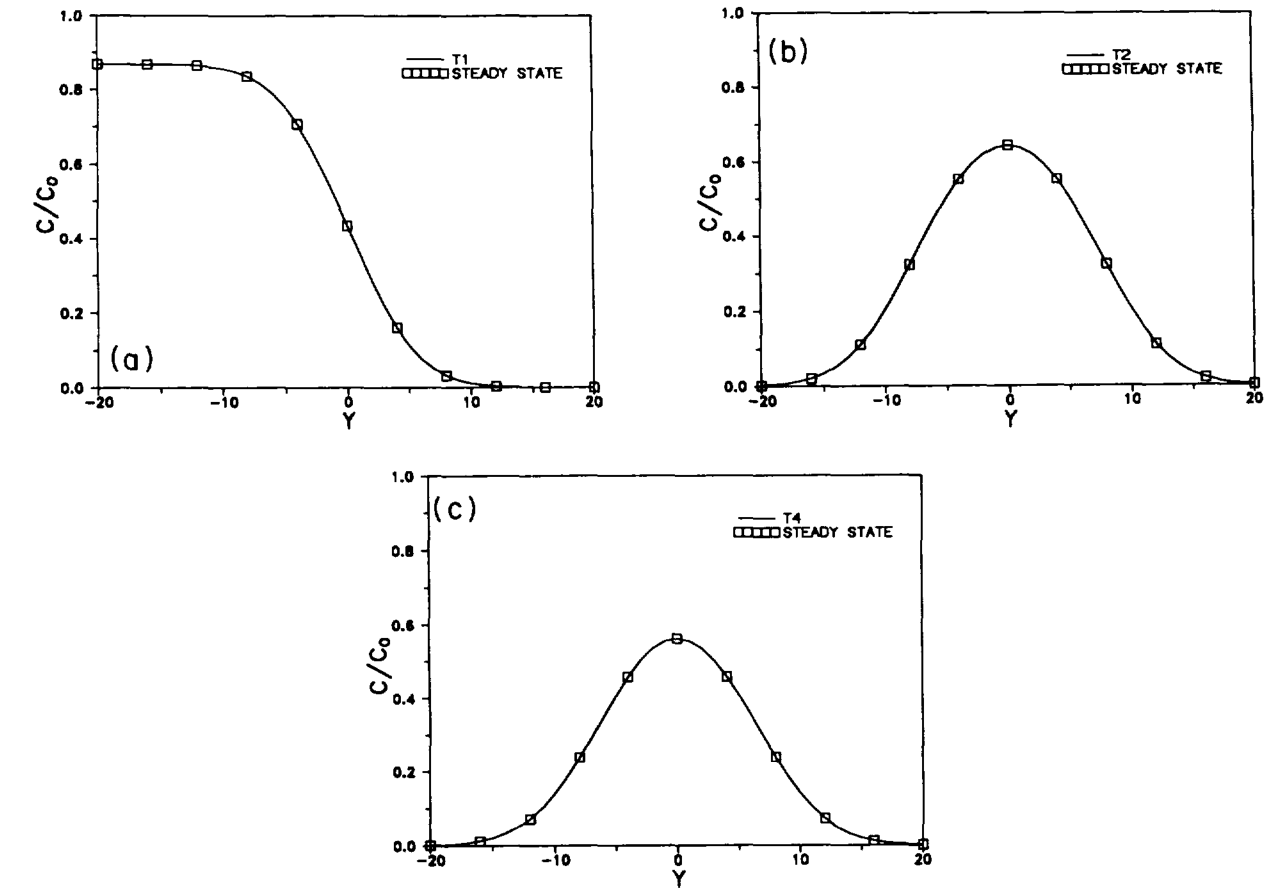

Fig. 2. Comparison of steady state solutions with results for (*a*) case 1, (*b*) case 2, and (*c*) case 4 at $t = 2$, $x = 50$, and $z = -5$ using $v = 50$, $D_x = 20$, $D_y = D_z = D_r = 10$, $\mu = \lambda = 0$, $R = 1$, and $a = b = 7.5$.

corresponds to the use of a first-type condition for flux-averaged concentrations. Therefore one can obtain first-type from third-type solutions, and vice versa, using the transformations [cf. *van Genuchten et al.*, 1984; *Batu and van Genuchten*, 1990]:

$$C_F = C_T - \frac{D_x}{v}\frac{\partial C_T}{\partial x} \tag{34a}$$

$$C_T = \frac{v}{D_x}\exp\left(\frac{vx}{D_x}\right)\int_x^\infty \exp\left(-\frac{v\xi}{D_x}\right)C_F(\xi)\,d\xi \tag{34b}$$

The subscripts F and T denote first- and third-type conditions, corresponding to flux- and volume-averaged concentrations, respectively. We verified that these transformations are consistent with solutions (19) and (31).

Second, the part of the solution that depends on y and z or r (i.e., the effect of transverse dispersion) is investigated. For cases 1, 2, and 4 we examined steady state transport while ignoring longitudinal dispersion [cf. *Harleman and Rumer*, 1963]. Such solutions may be useful to determine the transverse dispersion coefficients experimentally. The following solutions were obtained:

Case 1

$$C(x, y, z) = \frac{C_o}{4}\,\mathrm{erfc}\left[\frac{y}{(4D_y x/v)^{1/2}}\right]\mathrm{erfc}\left[\frac{z}{(4D_z x/v)^{1/2}}\right] \tag{35}$$

Case 2

$$C(x, y, z) = \frac{C_o}{4}\left[\mathrm{erfc}\left(\frac{y-a}{(4D_y x/v)^{1/2}}\right) - \mathrm{erfc}\left(\frac{y+a}{(4D_y x/v)^{1/2}}\right)\right] \cdot \left[\mathrm{erfc}\left(\frac{z-b}{(4D_z x/v)^{1/2}}\right) - \mathrm{erfc}\left(\frac{z+b}{(4D_z x/v)^{1/2}}\right)\right] \tag{36}$$

Case 4

$$C(x, r) = \int_0^a \frac{v\rho C_o}{2D_r x}\exp\left(-\frac{v(r^2+\rho^2)}{4D_r x}\right)\mathrm{I}_0\left(\frac{vr\rho}{2D_r x}\right)d\rho \tag{37}$$

Figure 2 shows the results for these steady state solutions, as well as the transverse concentration profiles calculated with the equations in Table 2 assuming large times. The correspondence between the two sets of solutions is excellent. Note that the difference between the use of a first- and third-type condition is negligible at large times.

Third, the effect of the inlet condition (first versus third type) is investigated. Consider the application of solute free water to an effectively one-dimensional medium where the solute is initially uniformly distributed between x_1 and x_2 (case 3 with a and b approaching infinity). The concentration profile is computed for various times using the two different inlet conditions. Figure 3 shows the results for $v = 50$ (3*a*) and $v = 0$ (3*b*) with the same hypothetical value for D_x at

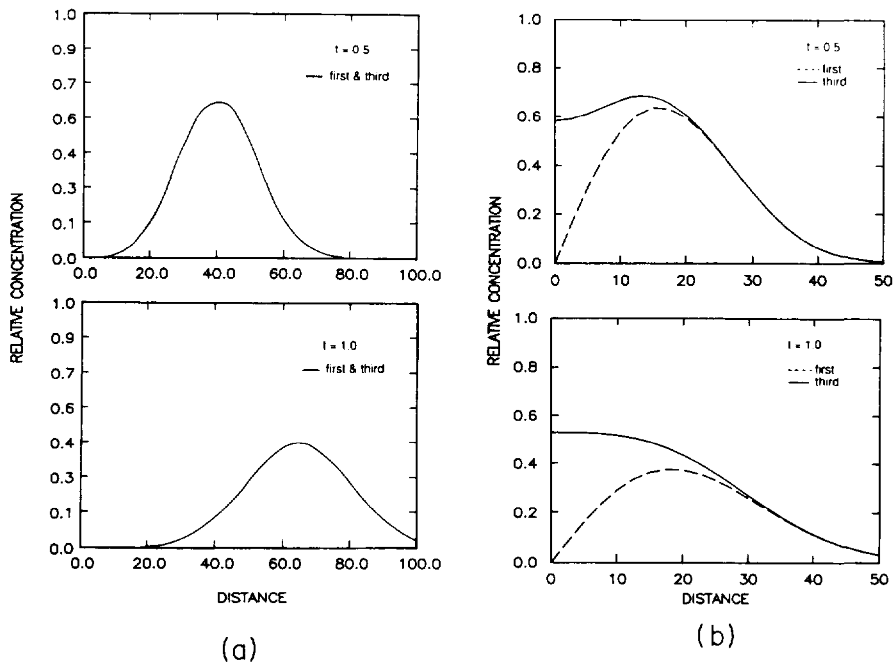

Fig. 3. Concentration versus depth, x, at $y = z = 0$ for $t = 0.5$ and $t = 1$ with $D_x = 100$, $D_y = D_z = 10$, $\mu = \lambda = 0$, $R = 1$, $x_1 = 5$ and $x_2 = 25$ and $a = b = 7.5$ for case T3 and F3 (using first- and third-type inlet conditions): (*a*) $\nu = 50$ and (*b*) $\nu = 0$.

$t = 0.5$ and 1. In the first case the first- and third-type concentration profiles are virtually identical whereas for no flow the differences between the two concentration profiles are substantial, particularly close to the inlet. The restriction that $C|_{x=0^+} = 0$ for a first-type condition results in lower predicted concentrations for a first than a third-type condition. To illustrate the effect of the inlet condition for a three-dimensional system, consider the application of solute over a rectangular area at the surface to an initially solute free soil using $D_x = 100$ and $\nu = 10$. Figure 4 shows concentration profiles in the transverse y direction for various values of x at $t = 1$ for a first- and third-type boundary condition. Notice that the first-type condition implies that $C|_{x=0^+} = C_o$, and that now the third-type condition predicts lower concentrations. For volume-averaged concentrations the first-type condition (dashed line) overestimates the amount of solute in the profile [cf. *van Genuchten and Parker*, 1984]. The error in the mass balance caused by improper use of boundary conditions will be pursued in the next section. Unless stated otherwise, we will, from now on, use only third-type inlet conditions.

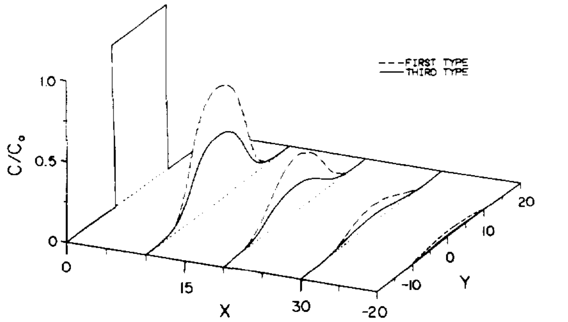

Fig. 4. Dimensionless concentration versus longitudinal and transverse direction (y) at $z = 0$ and $t = 1$ for cases F2 (first type) and T2 (third type) using $\nu = 10$, $D_x = 100$, $D_y = D_z = 10$, $\mu = \lambda = 0$, $R = 1$, and $a = b = 7.5$.

Fourth, the ADE is reduced to the classical heat or diffusion equation by assuming that $\nu = 0$. Concentration profiles were derived for case 3 where the solute was incorporated between x_1 and x_2. Figure 5 illustrates solute movement as a result of diffusion from the "buried" solute source. In Figure 5*a* the concentration is plotted versus depth (x) and in the transverse direction (y), whereas Figure 5*b* contains solute concentration profiles in the xy plane. Because the source is located close to the surface, a nonsymmetrical solute profile develops in the x direction.

The last part of this section includes some illustrative examples. Consider again the spreading of a solute initially confined to a parallelepipedal area of the soil (case 3). In Figure 6*a* the solute concentration is plotted versus depth below the soil surface (x) and the transverse direction (y) for different times. The concentration profile is in this example also symmetrical to the x direction. A reduction in the maximum concentration and the increased longitudinal and lateral spreading of the solute with increasing time can clearly be observed. Figure 6*b* provides a planar view of a soil section with lines of equal concentrations as contours corresponding to the times given in Figure 6*a*.

The following two examples deal with radial transport. Figure 7*a* shows the development of a solute plume as a result of solute application from a circular area at the soil

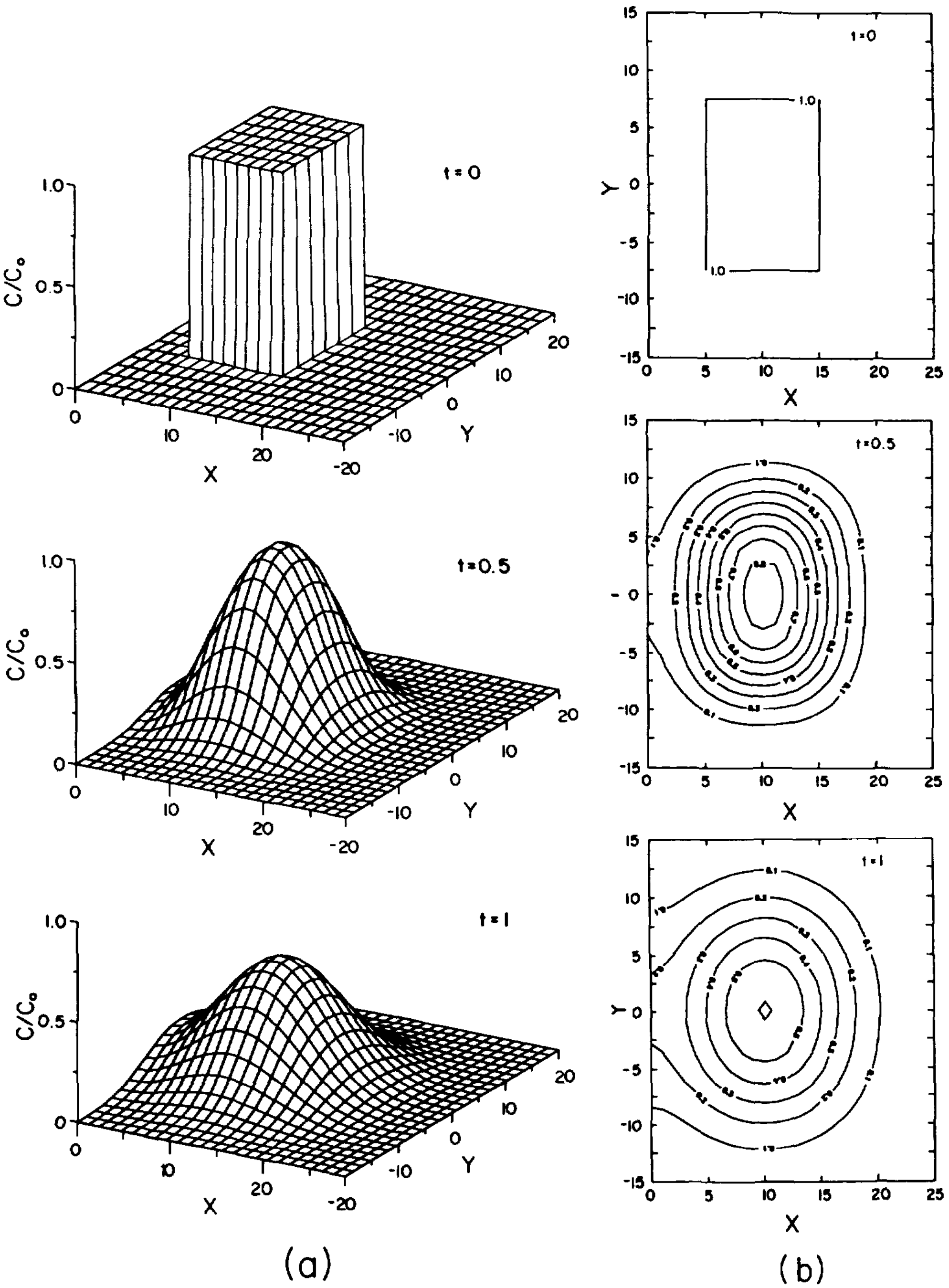

Fig. 5. Concentration distributions obtained for case T3 at $z = 0$ for $t = 0$, $t = 0.5$, and $t = 1$ with $\nu = 0$, $D_x = D_y = D_z = 10$, $\mu = \lambda = 0$, $R = 1$, $a = b = 7.5$, $x_1 = 5$ and $x_2 = 15$: (*a*) C/C_o plotted as a function of x and y and (*b*) lines of equal C/C_o plotted in the xy plane.

surface (case 4), whereas Figure 7*b* gives contours of the concentration in the radial plane for different depths. Figure 8 provides similar information for case 5, which assumes that the solute is initially present in a cylindrical region of the soil.

Thus far we assumed that zero- and first-order rate processes could be ignored ($\lambda = \mu = 0$). It is of interest to examine the influence of zero-order production and first-order decay on the solute distribution. Concentration distributions were determined for cases T1 and T3 using similar values for λ and μ as *van Genuchten* [1981]. Figure 9 contains the results for case T2 using different values for the production term, λ, and no decay (Figure 9*a*) or various decay rates, μ, without production (Figure 9*b*). As can be expected, greater values for λ and μ cause increases and decreases in concentration, respectively. Figure 10 shows similar curves for case T3. The curves correspond to those presented by *van Genuchten* [1981]. Note that we assumed positive values for λ and μ. The source term λ can be immediately transformed into a sink by using negative values. A similar change in sign is possible for the decay rate μ.

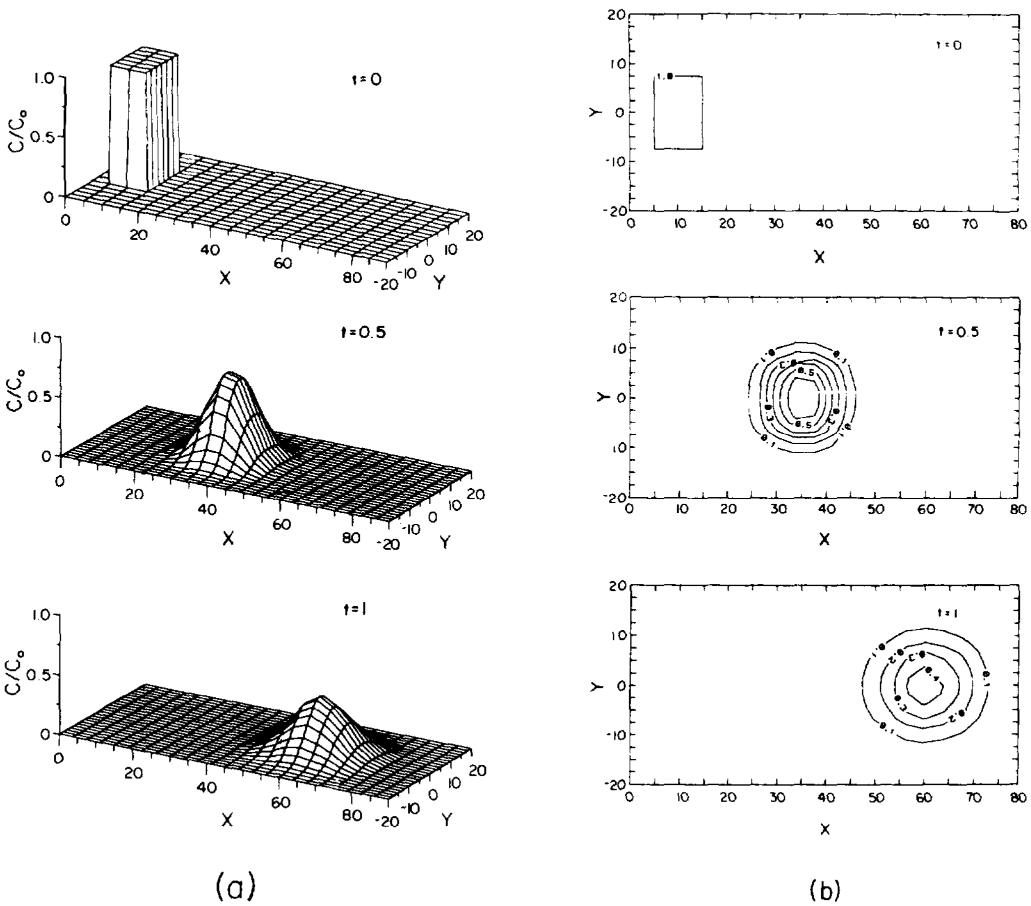

Fig. 6. Concentration distributions obtained for case T3 at $z = 0$ for $t = 0$, $t = 0.5$, and $t = 1$ with $\nu = 50$, $D_x = 20$, $D_y = D_z = 10$, $\mu = \lambda = 0$, $R = 1$, $a = b = 7.5$, $x_1 = 5$ and $x_2 = 15$: (*a*) C/C_o plotted as a function of x and y and (*b*) lines of equal C/C_o plotted in the xy plane.

The above examples illustrate the usefulness of analytical solutions for predicting or simulating solute movement. The solutions may also be used for determining transport parameters from solute displacement experiments with nonlinear curve-fitting techniques [e.g., *Kool et al.*, 1987].

MASS BALANCE CONSTRAINTS

A secondary objective of this study was to investigate mass balance constraints and to formulate potential errors when improper boundary conditions are applied for the analytical solution (notably the first- and third-type inlet conditions). To formulate the mass balance constraint for steady water flow, we assume that the amount of solute entering the soil is determined solely by advection in the influent solution. Following *van Genuchten and Parker* [1984], the relative mass balance "error" for cases 1, 2, and 4 is [cf. *Batu and van Genuchten*, 1990]:

$$E_r = \frac{R\int_0^\infty\int_{-\infty}^\infty\int_{-\infty}^\infty C(x, y, z, t)\, dy\, dz\, dx}{\int_0^t\int_{-\infty}^\infty\int_{-\infty}^\infty \nu C(0, y, z, t)\, dy\, dz\, dt} - 1 \qquad (38)$$

while for cases 3 and 5 (i.e., solute incorporated in the soil profile) the error can be defined as:

$$E_r = \frac{\int_0^\infty\int_{-\infty}^\infty\int_{-\infty}^\infty C(x, y, z, t)\, dy\, dz\, dx)}{\int_0^\infty\int_{-\infty}^\infty\int_{-\infty}^\infty C(x, y, z, 0)\, dy\, dz\, dx} - 1 \qquad (39)$$

To investigate differences in the use of a first- and a third-type condition we will obtain expressions for E_r for cases 2 and 3 using both inlet conditions, and assuming $\mu = \lambda = 0$.

First, examine the case of solute application to an initially solute-free soil profile. After substitution of solution F2 into (38) and subsequent integration we obtained

$$E_r = \frac{1}{2\zeta\sqrt{\pi}} \exp\left(-\frac{\zeta^2}{2}\right) + \frac{1}{2\zeta^2} - \left(\frac{1}{2\zeta^2} + \frac{1}{2}\right) \operatorname{erfc}(\zeta) \qquad (40)$$

where

$$\zeta = \sqrt{\frac{\nu^2 t}{4RD_x}} \qquad (41)$$

This expression is identical to (10) of *van Genuchten and Parker* [1984]; the first-type condition overestimates the total amount of solute in the soil profile. The similarity shows that the mass balance error is not affected by transverse disper-

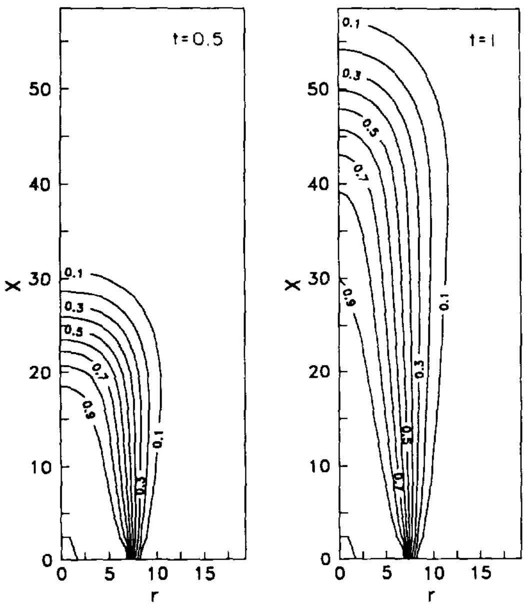

(a)

Fig. 7. Concentration distributions obtained for case T4 with $v = 50$, $D_x = 20$, $D_r = 10$, $\mu = \lambda = 0$, $R = 1$, and $a = 7.5$: (*a*) concentration contours in the xr plane at $t = 0.5$ and 1 and (*b*) concentration contours in the transverse yz plane at $t = 1$.

sion, nor by the geometry of the application area in our study. In a similar fashion we derived that $E_r = 0$, as it should be, for solution T2. These results correspond to the findings by *Batu and van Genuchten* [1990] for two-dimensional transport. Figure 11 shows the value of E_r as a function of ζ for a first-type condition.

Now consider application of solute free water to a soil with a uniform initial distribution in a parallelepiped with lengths $2a$, $2b$, and $x_2 - x_1$ (case 3). The mass balance error was obtained by integrating (13) with respect to x and applying $\mathcal{L}_t^{-1}$ and $\mathcal{F}_{yz}^{-1}$, respectively. The expression for E_r was subsequently obtained according to (39). For a first-type condition E_r is given by

$$E_r = \frac{1}{2(\omega_2 - \omega_1)} \left\{ \left(\omega_1 + \zeta + \frac{1}{4\zeta} \right) \operatorname{erfc} [\omega_1 + \zeta] - \left(\omega_2 + \zeta + \frac{1}{4\zeta} \right) \operatorname{erfc} [\omega_2 + \zeta] + \frac{1}{\sqrt{\pi}} \cdot (\exp [-(\omega_2 + \zeta)^2] - \exp [-(\omega_1 + \zeta)^2]) + \frac{1}{4\zeta} (\exp (-4\zeta \omega_2) \operatorname{erfc} [\omega_2 - \zeta] - \exp (-4\zeta \omega_1) \operatorname{erfc} [\omega_1 - \zeta]) \right\} \tag{42}$$

where

$$\omega_i = \sqrt{\frac{R x_i^2}{4 D_x t}} \qquad (i = 1, 2) \tag{43}$$

The error is again not influenced by transverse dispersion but does depend on the locations x_1 and x_2. For a third-type condition we verified that $E_r = 0$. The "error" for a first-type condition (42) was plotted as a function of ω_1 and ω_2 for various ζ in Figure 12. The error can be quite significant for small values of ω_1 and ζ if the solute is initially present in a region close the soil surface (i.e., $x_2 - x_1$ is small). The first-type condition underestimates the total amount of solute in the soil since it permits backdiffusion through the soil surface (this condition does not stipulate a "zero flux" at $x = 0$). However, results suggest that for most practical cases the value for E_r will be relatively small.

SUMMARY AND CONCLUSIONS

Solute transport in semi-infinite homogeneous porous media was modeled analytically for one-dimensional flow assuming linear retardation, a zero-order sink/source term, a first-order production/decay term, and using a first- or third-type condition at the inlet. The governing partial differential equation was solved in a straightforward manner for general inlet and initial solute distributions by applying a Laplace transform with respect to x and t, a double Fourier trans-

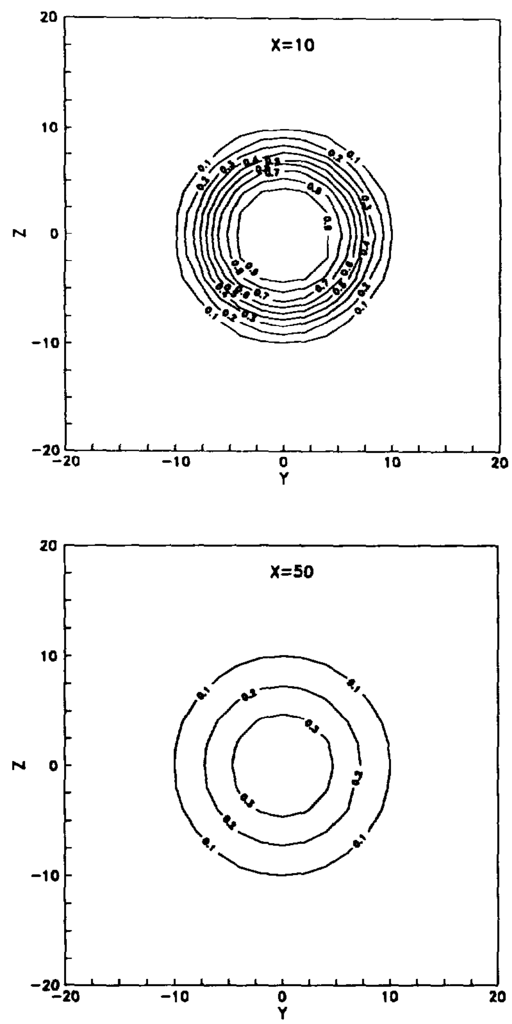

(b)

Fig. 7. (continued)

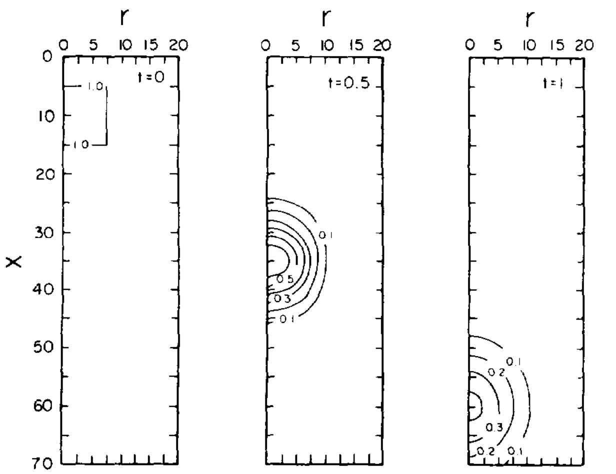

Fig. 8. Concentration contours in the xr plane at t = 0, 0.5, and 1 for case T5 with $\nu = 50$, $D_x = 20$, $D_r = 10$, $\mu = \lambda = 0$, $R = 1$, $x_1 = 5$ and $x_2 = 15$, and $a = 7.5$.

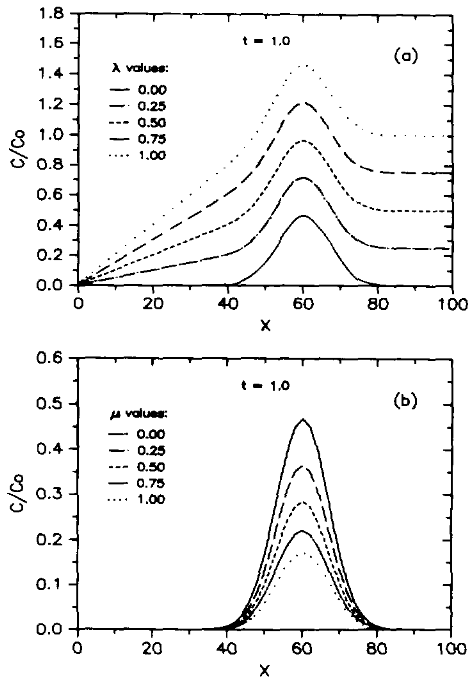

Fig. 10. Concentration distribution for case T3 with $x_1 = 5$ and $x_2 = 15$, and $a = b = 7.5$ at $t = 1$, and $z = y = 0$ using $\nu = 50$, $D_x = 20$, $D_y = D_z = 10$, and $R = 1$: (a) different production terms and zero decay and (b) different decay rates and zero production.

form with respect to y and z for a Cartesian coordinate system, and a Hankel transform for a cylindrical coordinate system. The solute concentration in the real space and time domain was obtained by solving the ensuing algebraic equation and applying the appropriate inverse integral transforms. The general solutions for the first- and third-type conditions were used to derive expressions for the concentration distribution for five specific cases.

Mass balance errors were derived for solute application from a rectangular area at the surface to an initially solute-free soil profile, as well as for application of solute-free water to a soil where the solute was initially uniformly distributed in a parallelepipedal area just below the soil surface. For solute application adoption of a first-type inlet condition was shown to lead to mass balance errors in terms of the volume-averaged concentration, whereas the analytical solution derived for a third-type condition obeyed the mass conservation principle. For a first-type condition, mass balance errors for the initial distribution of the solute depended on the position below the soil surface where the solute was initially present. Solutions obtained for third-type conditions again conserved mass.

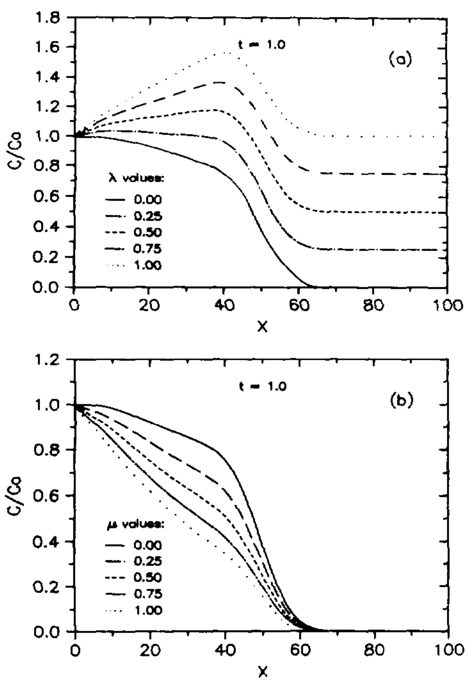

Fig. 9. Concentration distribution for case T1 at $t = 1$, $z = y = -5$ using $\nu = 50$, $D_x = 20$, $D_y = D_z = 10$, and $R = 1$: (a) different production terms and zero decay and (b) different decay rates and zero production.

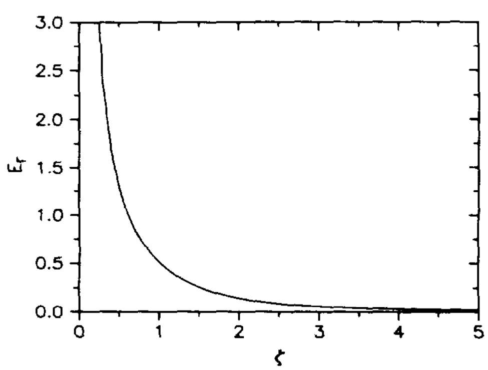

Fig. 11. Relative mass balance error E_r versus ζ for case F2.

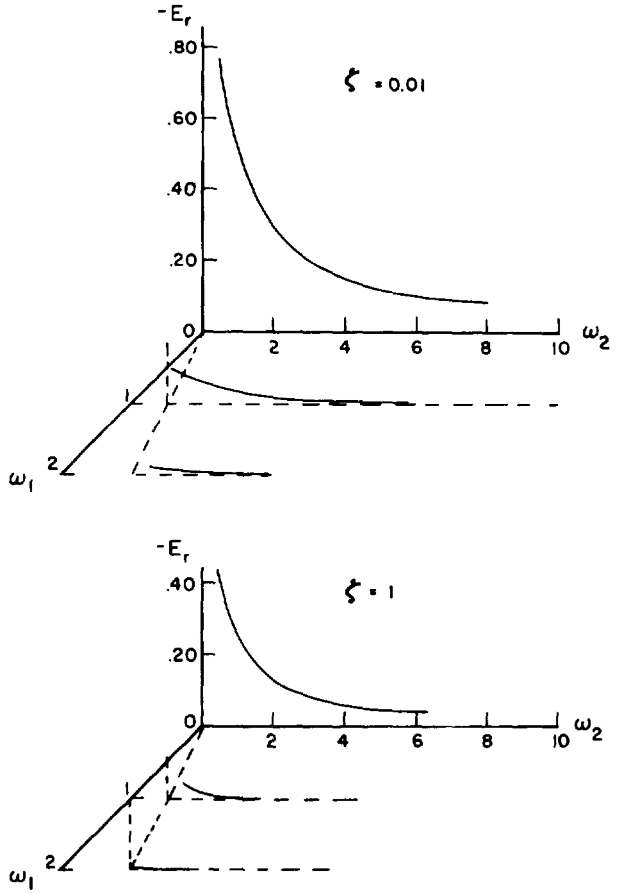

Fig. 12. Relative mass balance error E_r versus ω_1 and ω_2 for various ζ for case F3.

APPENDIX: EVALUATION OF VARIABLES IN (12)

For the first-type condition, $d\bar{C}^{yz}/dx(0, \alpha, \beta, s)$ needs to be evaluated, whereas for a third-type condition $\bar{C}^{yz}(0, \alpha, \beta, s)$ should be known. This is accomplished by using outlet condition (4). Differentiation of (12) yields

$$\frac{d\bar{C}^{yz}}{dx}(x, \alpha, \beta, s) = [(1-\delta)\bar{g}^{yz} + \delta\bar{C}^{yz}(0, \alpha, \beta, s)]$$

$$\cdot \frac{\exp(-Ax)}{B}\{(B^2 + A^2)\sinh(Bx) - 2AB\cosh(Bx)\}$$

$$+ \left[(1-\delta)\frac{d\bar{C}^{yz}}{dx}(0, \alpha, \beta, s) - \frac{\nu\bar{g}^{yz}}{D_x}\right]\frac{\exp(-Ax)}{B}$$

$$\cdot \{B\cosh(Bx) - A\sinh(Bx)\} + \frac{R}{BD_x}$$

$$\cdot \int_0^x \left[f^{yz}(\xi, \alpha, \beta) + \frac{\lambda^{yz}}{Rs}\right]\exp[-A(x-\xi)]$$

$$\cdot \{A\sinh[B(x-\xi)] - B\cosh[-A(x-\xi)]\}\, d\xi \qquad \text{(A1)}$$

where differentiation of the integral was carried out with Leibnitz' rule. Converting cosh and sinh to exponential form and multiplying (A1) by $2B\exp[(A-B)x]$ leads to

$$2B\exp[(A-B)x]\frac{d\bar{C}^{yz}}{dx} = [(1-\delta)\bar{g}^{yz} + \delta\bar{C}^{yz}(0, \alpha, \beta, s)]$$

$$\cdot \{(B^2 + A^2)[1 - \exp(-2Bx)] - 2AB[1 + \exp(-2Bx)]\}$$

$$+ \left[(1-\delta)\frac{d\bar{C}^{yz}}{dx}(0, \alpha, \beta, s) - \frac{\nu\bar{g}^{yz}}{D_x}\right]$$

$$\cdot \{B[1 + \exp(-2Bx)] - A[1 - \exp(-2Bx)]\} + \frac{R}{D_x}$$

$$\cdot \int_0^x \left[f^{yz}(\xi, \alpha, \beta) + \frac{\lambda^{yz}}{Rs}\right]\exp(A\xi)\{A[\exp(-B\xi)$$

$$- \exp(B(\xi - 2x))] - B[\exp(-B\xi)$$

$$+ \exp(B(\xi - 2x))]\}\, d\xi \qquad \text{(A2)}$$

Taking $x \to \infty$, using (4) and dividing by $(B - A)$ leads to

$$[(1-\delta)\bar{g}^{yz} + \delta\bar{C}^{yz}(0, \alpha, \beta, s)](B - A)$$

$$+ \left[(1-\delta)\frac{d\bar{C}^{yz}}{dx}(0, \alpha, \beta, s) - \frac{\nu\bar{g}^{yz}}{D_x}\right]$$

$$- \frac{R}{D_x}\int_0^x \left[f^{yz}(\xi, \alpha, \beta) + \frac{\lambda^{yz}}{Rs}\right]\exp[\xi(A - B)]\xi = 0$$

$$\text{(A3)}$$

Hence, for a first-type condition ($\delta = 0$),

$$\frac{d\bar{C}^{yz}}{dx}(0, \alpha, \beta, s) = \frac{R}{D_x}\int_0^x \left(f^{yz}(\xi, \alpha, \beta) + \frac{\lambda^{yz}}{Rs}\right)$$

$$\cdot \exp[\xi(A - B)]\, d\xi - (A + B)\bar{g}^{yz} \qquad \text{(A4)}$$

and for a third-type condition ($\delta = 1$),

$$\bar{C}^{yz}(0, \alpha, \beta, s) = \frac{1}{(B - A)D_x}\left\{\nu\bar{g}^{xy} + \int_0^x \left(Rf^{yz}(\xi, \alpha, \beta)\right.\right.$$

$$\left.\left. + \frac{\lambda^{yz}}{s}\right)\exp[\xi(A - B)]\, d\xi\right\} \qquad \text{(A5)}$$

REFERENCES

Abramowitz, M., and I. A. Stegun (Eds.), *Handbook of Mathematical Functions, Appl. Math. Ser.*, vol. 55, National Bureau of Standards, Washington, D. C., 1970.

Batu, V., and M. Th. van Genuchten, First- and third-type boundary conditions in two-dimensional solute transport modeling, *Water Resour. Res.*, *26*, 339–350, 1990.

Bear, J., *Hydraulics of Groundwater*, McGraw-Hill, New York, 1979.

Bruch, J. C., and R. L. Street, Two-dimensional dispersion, *J. Sanit. Eng. Div. Proc. Am. Soc. Civ. Eng.*, *93*(SA6), 17–39, 1967.

Carnahan, C. L., and J. S. Remer, Nonequilibrium and equilibrium sorption with a linear sorption isotherm during mass transport through an infinite porous medium: Some analytical solutions, *J. Hydrol.*, *73*, 227–258, 1984.

Carslaw, H. S., and J. C. Jaeger, *Conduction of Heat in Solids*, Oxford University Press, New York, 1959.

Chen, C.-S., Analytical solutions for radial dispersion with Cauchy boundary at injection well, *Water Resour. Res.*, *23*, 1217–1224, 1987.

Cleary, R. W., Unsteady-state, multi-dimensional analytical modeling of water quality in rivers, *Water Resour. Prog. Tech. Rep. 1-73-1*, Dep. of Civ. Eng., Princeton Univ., Princeton, N. J., 1973.

Cleary, R. W., and M. J. Ungs, Analytical methods for ground water pollution and hydrology, *Water Resour. Prog. Rep. 78-WR-15*, Dep. of Civ. Eng., Princeton Univ., Princeton, N. J., 1978.

Harleman, D. R. F., and R. R. Rumer, Longitudinal and lateral dispersion in an isotropic porous medium, *J. Fluid Mech.*, *16*, 385–394, 1963.

Javandel, I., C. Doughty, and C. F. Tsang (Eds.), *Groundwater Transport: Handbook of Mathematical Models, Water Resour. Monogr. Ser.*, vol. 10, AGU, Washington, D. C., 1984.

Kool, J. B., J. C. Parker, and M. Th. van Genuchten, Parameter estimation for unsaturated flow and transport models—A review, *J. Hydrol.*, *91*, 255–293, 1987.

Kuo, E. Y. T., Analytical solution for 3-D diffusion model, *J. Environ. Eng. Div. Proc. Am. Soc. Civ. Eng.*, *102*(EE4), 805–820, 1976.

Leij, F. J., and J. H. Dane, Analytical solution of the one-dimensional advection equation and two- or three-dimensional dispersion equation, *Water Resour. Res.*, *26*, 1475–1482, 1990.

Leij, F. J., J. H. Dane, and M. Th. van Genuchten, A mathematical analysis of one-dimensional solute transport in a layered soil profile, *Soil Sci. Soc. Am. J.*, in press, 1991.

Lindstrom, F. T., and L. Boersma, A theory on the mass transport of previously distributed chemicals in a water saturated sorbing porous medium, *Soil Sci.*, *111*, 192–199, 1971.

Lindstrom, F. T., and L. Boersma, Two-dimensional transport and fate of chemicals emitted by arbitrarily placed sources in confined aquifers, *Water Resour. Res.*, *25*, 1748–1756, 1989.

Moltyaner, G. L., and R. W. D. Killey, Twin Lake tracer tests: Longitudinal dispersion, *Water Resour. Res.*, *24*, 1613–1627, 1988.

Ogata, A., Two-dimensional dispersion in a granular-medium disk source emitting at constant rate, *U.S. Geol. Surv. Prof. Pap., 650-D*, 260–264, 1969.

Prakash, A., Ground-water contamination due to transient sources of pollution, *J. Hydraul. Div. Proc. Am. Soc. Civ. Eng.*, *110*(HY11), 1642–1658, 1984.

Press, W. H., B. P. Flannery, S. A. Teukolsky, and W. T. Vetterling, *Numerical Recipes*, Cambridge University Press, New York, 1986.

Sagar, B., Dispersion in three dimensions: approximate analytic solutions, *J. Hydraul. Div. Proc. Am. Soc. Civ. Eng.*, *108*(HY1), 47–62, 1982.

Shen, H. T., 1976, Transient dispersion in uniform porous media flow, *J. Hydraul. Div. Proc. Am. Soc. Civ. Eng.*, *102*(HY6), 707–716, 1976.

Sneddon, I. H., *The Use of Integral Transforms*, McGraw-Hill, New York, 1972.

Spiegel, M. R., *Theory and Problems of Laplace Transforms*, Schaum's Outline Ser., McGraw-Hill, New York, 1965.

Tang, D. E., and D. W. Peaceman, New analytical and numerical solutions for the radial convection-dispersion problem, paper presented at the Ninth Symposium on Reservoir Simulation, Soc. of Petrol. Eng., San Antonio, Tex., 1987.

van Genuchten, M. Th., Analytical solutions for chemical transport with simultaneous adsorption, zero-order production and first-order decay, *J. Hydrol.*, *49*, 213–233, 1981.

van Genuchten, M. Th., and W. J. Alves, Analytical solutions of the one-dimensional convective-dispersive solute transport equation, *Tech. Bull. U.S. Dep. Agric.*, *1661*, 1982.

van Genuchten, M. Th., and J. C. Parker, Boundary conditions for displacement experiments through short laboratory soil columns, *Soil Sci. Soc. Am. J.*, *48*, 703–708, 1984.

van Genuchten, M. Th., D. H. Tang, and R. Guennelon, Some exact solutions for solute transport through soils containing large cylindrical macropores, *Water Resour. Res.*, *20*, 335–346, 1984.

Wexler, E. J., Analytical solutions for one-, two-, and three-dimensional solute transport in ground-water systems with uniform flow, *U.S. Geol. Surv. Rep.*, *89-56*, 1989.

Wilson, J. L., and P. L. Miller, Two-dimensional plume in uniform ground-water flow, *J. Hydraul. Div. Proc. Am. Soc. Civ. Eng.*, *104*(HY4), 503–514, 1978.

Yeh, G.-T., and Y.-J. Tsai, Analytical three-dimensional transient modeling of effluent discharges, *Water Resour. Res.*, *12*, 533–540, 1976.

F. J. Leij and M. Th. van Genuchten, U.S. Salinity Laboratory, 4500 Glenwood Drive, Riverside, CA 92501.

T. H. Skaggs, Department of Soil and Environmental Science, University of California, Riverside, CA 92521.

(Received March 27, 1991;
revised July 8, 1991;
accepted July 18, 1991.)